

Analytical and experimental determination of the fracture toughness by means of small punch test specimens notched with a femtolaser

I. Peñuelas^{1,a}, C. Rodríguez^{1,b}, F.J. Belzunce^{1,c}, C. Betegón^{1,d}

¹ Instituto Universitario de Tecnología Industrial de Asturias (IUTA). University of Oviedo. Campus Universitario. 33203 Gijón. Spain

penuelasines@uniovi.es, cristina@uniovi.es, belzunce@uniovi.es, cova@uniovi.es

Keywords: Miniature tests, small punch test, fracture toughness.

Abstract. Knowledge of the mechanical properties of structural components and their degradation during long-term services are key factors in assessing the structural integrity of any facility and its residual life. As conventional mechanical characterization of materials (with the exception of hardness) is always destructive, the use of miniature tests is considered to be very interesting if suitable specimens can be extracted from real components without affecting their operating capacity. In this paper, micromachined, laser and femtolaser notched SPT specimens were tested, experimentally determining the load for the initiation of the crack growth, modelling the entire SPT experiment by means of finite element (FE) simulation and calculating the J value for the initiation of crack growth. The obtained results were compared with the results also obtained by means of standard J_{Ic} tests performed on single edge notch bend (SE[B]) specimens. The femtolaser technique allows to obtain notches much sharper than those obtained using other techniques such as micromachining or laser, without causing apparent damage to the material close to the notch.

Introduction

The characterization of the mechanical behaviour of structural materials, with the exception of material hardness, is a destructive procedure which requires direct extraction of test specimens from the component to analyse. Since components need to be operative, these specimens have to be as small as possible, in order not to affect the behaviour of the components and in order to allow easy repair of the ‘damaged’ components. However, tests with miniaturized specimens are not defined in standards. Thus, the results obtained with these tests have to be interpreted in order to obtain the actual properties of the components from which the specimens have been extracted [1]. The small punch test (SPT) is very useful in all applications that require the characterization of the mechanical behaviour of structural materials or operational components without compromising their service [2], as in the case of nuclear or thermal plants. Another application is the study of small testing zones. Thus, this test has been recently applied to the mechanical characterization of metallic coatings [3,4] or the heat affected zone of welds [5], which are practically impossible to characterize by means of the conventional mechanical tests. The macromechanical and micromechanical parameters relate with different zones of the load-displacement curve obtained with the SPTs.

The SPT was first used in the nuclear industry to show the evolution of materials submitted to irradiation [4,6] It was shown to enable the obtaining of quite reliable conventional mechanical properties (yield strength, ultimate tensile strength and ductile-to-brittle transition temperature) [7,8,9,10]. Subsequently, several authors [10,11,12,13] have tried to obtain fracture parameters (K_{Ic} , fracture energy, damage parameters) using the same type of specimens. However, although some promising results have been obtained, there is still no experimental procedure able to predict the fracture toughness of a ductile metallic material from the small punch test. Moreover, given that the

fracture toughness is the energy required to initiate the growth of a pre-existing crack, it would appear that a notched or cracked specimen is required to obtain accurate results.

Different notched SPT specimens were tested in this study, experimentally determining the load for the initiation of the crack growth, modelling the entire SPT experiment by means of finite element simulation and calculating the J value for the initiation of crack growth. The obtained result was compared with the result also obtained by means of a standard J_{Ic} test performed on single edge notch bend (SE(B)) specimens.

Small Punch Test

The specimens used for the SPT are usually square plates of $10 \times 10 \text{ mm}^2$ and just 0.5 mm thickness, although lower or higher thickness can also be used. In comparison with other non-destructive techniques such as ultrasonic or magnetic techniques and X-Rays, that are based on indirect measures for the determination of the above mentioned properties, the SPT allows obtaining directly the main mechanical properties of the materials.

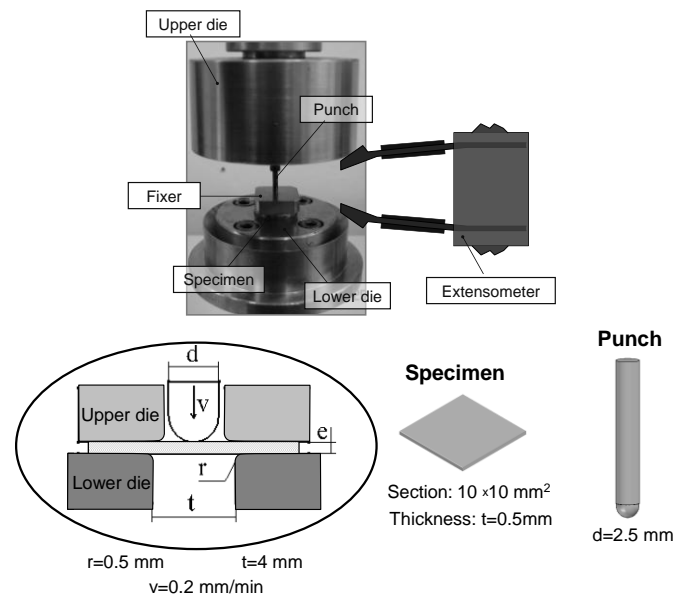


Fig. 1. Dispositive and geometry of the small punch test

In laboratory, the SPTs have been carried out with a low speed tensile test machine coupling a special device designed and manufactured in the Polytechnic Engineering School of Gijón, Spain, to a universal Instron 5582 machine. The $10 \times 10 \text{ mm}$ SPT specimens were cut by means of a precision metallographic cutting machine from slices of 0.5 mm thickness produced by electro-discharge machining. Test consists of fixing the periphery of the specimen, embedding it between two dies (upper and lower dies) by means of four screws and a tightening torque of 2 N·m, and then deforming the specimen until its fracture by means of a small semi-spherical punch with a head of 2.5 mm of diameter. The test is speed controlled with a punching speed $v = 0.2 \text{ mm/min}$. In this way, the specimen is bounded to deform quasi-statically inside a 4 mm diameter hole (biaxial expansion) up to failure (Fig. 1). The data sampling rate during the experiment is 20 specimens/s. Moreover, the test is finalized when load decreases the 50% of the maximum load. By means of a COD extensometer, the displacement of the punch is obtained, and after correction of the flexibility of the testing device, the displacement of the central point of the specimen is calculated. Thus, from test is obtained the characteristic curve of the material. This curve represents the force exerted from

punch against the specimen (i.e. the load reaction) versus the displacement of the punch (Fig. 2). In the case of ductile materials, six different zones can be distinguished in these load-displacement curves obtained by means of the SPTs: zone I (elastic deformation), zone II (elastoplastic transition), zone III (generalized plastic deformation), zone IV (plastic instability and fracture initiation), zone V (fracture softening zone) and zone VI (final fracture).

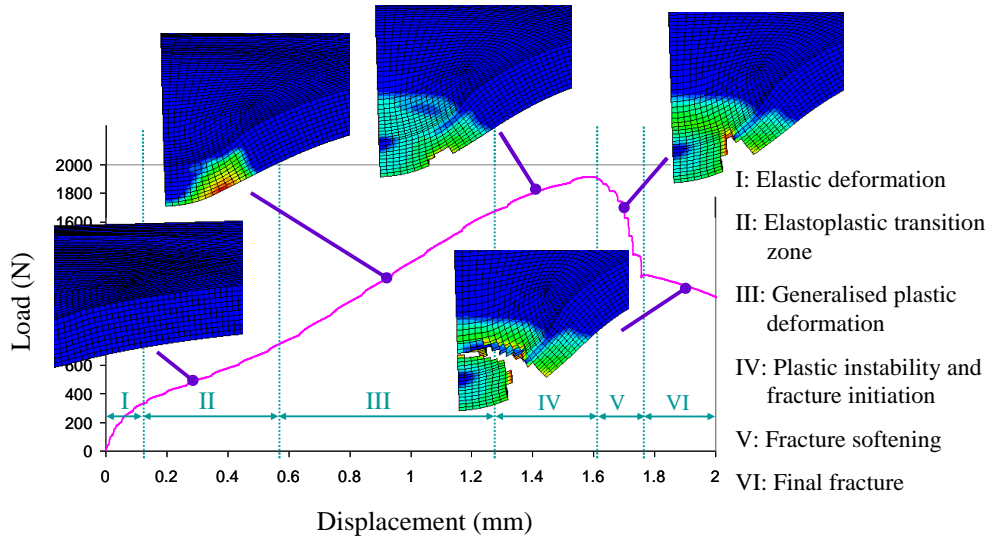


Fig. 2. Load-displacement curve for the SPT and Finite Element simulation at each zone (un-notched specimen)

Small Punch Test in notched specimens

As it was pointed out before, notched or cracked SPT specimens are required to obtain the fracture parameters. In previous papers [12] the authors studied the optimum configuration of the notch for determining the fracture toughness in metallic materials, by means an analysis of the stress triaxiality found in the notch tip. In these studies, numerical simulations were developed, using SPT specimens with 0.5 mm and 1 mm thickness, and different geometries and relative depths $a/t=0.1, 0.2, 0.3, 0.4, 0.5$ y 0.6 , with a the depth of the notch and t the thickness of the specimen, $e=cte$, and three different configurations: a) specimen with longitudinal notch (L); b) specimen with longitudinal and transversal notch (L+T); c) specimen with circular notch (C) of 3mm of diameter – see Fig. 3.

In all cases the geometry of the simulated notches corresponded to laboratory micromachined notches specimens. Using this technique, the minimum radius achieved at the tip of the notch was $100\ \mu\text{m}$. Fig. 4-left shows a detail of the notch obtained by micromachining, its important to observe the good surface finish obtained on the lips of the notch. The numerical results were compared with experimental results obtained interesting results. From the different configurations studied, the most appropriate one for determining the fracture toughness was L-configuration. In the case of notched specimens, interrupted laboratory tests were performed at different percentages of the maximum load, in order to determine when the crack starts to grow. With this data and numerical simulations the value of the integral J initiation of crack growth (J_{IC}) was obtained. This value was compared with that obtained by conventional tests on SE(B) specimens [14].

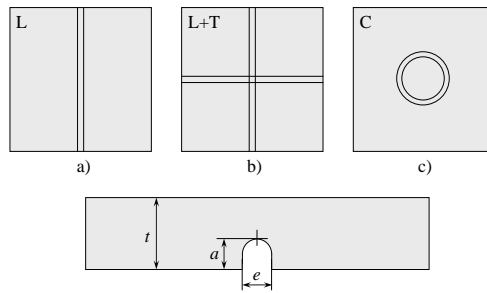


Fig. 3. Notches configurations analysed and a/t relation

Fig. 5 compares the X-70TT load-displacement curve obtained with a smooth (un-notched) and a notched specimen of similar thickness. The type of graph is quite similar, although maximum load and displacement significantly decrease when a crack is provided

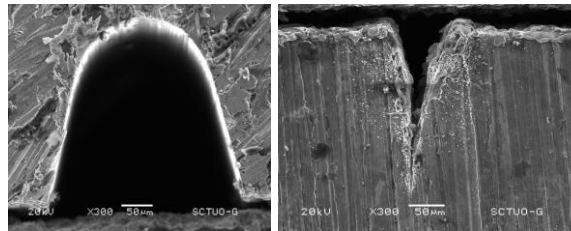


Fig. 4. Detail of the notch tip obtained by micromachining (left) and by laser (right)

Notwithstanding, since there is a big difference between the notch tip in the conventional specimens and that obtained in SP notched specimens by means of micromachining, all the procedure was repeated again with laser-notched specimens (with notch tip radius of $10\ \mu\text{m}$) and that obtained by laser varies. This geometry of the notch seems, a priori, more appropriate to determine the fracture toughness than the former one (micromachined-notch). Fig. 4-right shows a detail of the notch obtained by laser. In the Fig. it can be observed how the lips of the notch show a worse surface finishing in the case of the laser-notched than in the micromachining-notched specimen.

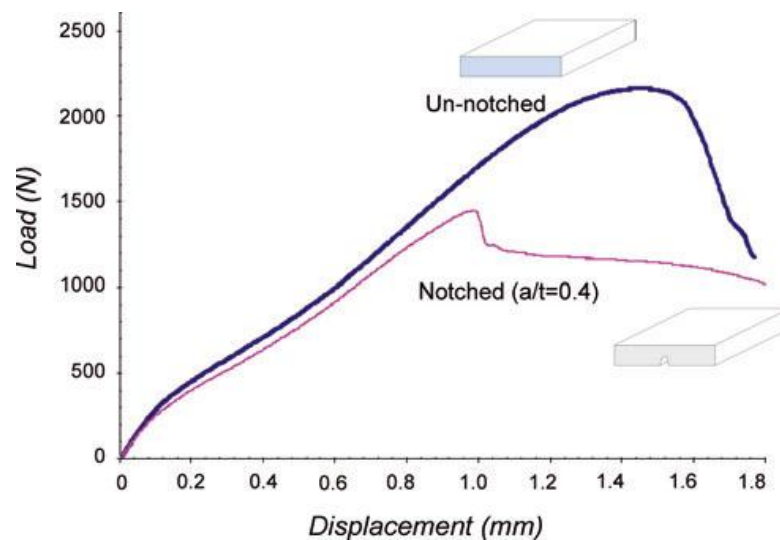


Fig. 5 Experimental load-displacement curves obtained on smooth (un-notched) and notched ($a/t = 0.4$) specimens of similar thickness (X-70TT).

Experimental procedure

A controlled rolled niobium and vanadium microalloyed API X-70 steel sheet with a thickness of 15 mm was employed in this experimental work. The chemical composition of the steel is: 12% C, 1.55% Mn, 0.23% Si, 0.003% S, 0.017% P, 0.049% Nb and 0.06% V. The steel sheet was butt welded using a 4.4 kW Nd-YAG laser (DY044 from ROFIN) at a weld velocity of 8 mm/s. Two passes were needed to attain total penetration. No preheating, post-heating or post-weld heat treatment was used. A transversal section of the welded coupon was ground, polished and etched with Nital to analyse the microstructure of the different regions of the weld and the hardness profile (Vickers hardness with a load of 10 kg). In addition, the coarse grain heat-affected zone was simulated by means of a suitable thermal treatment (X-70-TT). A 200x120x15 mm block was heated in a laboratory furnace to 1100°C for 45 minutes and subsequently cooled in still water. The microstructure and hardness of this product was also measured. The mechanical properties of the simulated coarse grain heat-affected zone were determined by means of standard tensile and fracture toughness tests (table 1). The tensile tests used cylindrical specimens with a diameter of 10 mm while the fracture toughness tests were performed on single edge notch bend specimens with long cracks ($a/W=0.5$) and a width and thickness of 14 mm, following the ASTM E1820 standard [15] to obtain the crack growth J-R resistant curves ($J-\Delta a$). The critical J_{Ic} value was defined at the intersection point between the experimental J-R curve and the blunting construction line at an offset value of 0.2 mm: hence, crack initiation actually corresponds to a true crack growth of 0.2 mm.

Table 1. Mechanical properties of the X70 TT steel

Steel	E GPa	σ_e MPa	σ_R MPa	e %	k MPa	n	J_{Ic} kJ/m ²
X-70TT	205	927	1259	13	1968	0.11	188

The determination of the conventional mechanical properties as well as the calculation of the fracture toughness of a material with elastoplastic behaviour: parameters $J_{Ic} = J_{\Delta a=0.2}^{\text{Standard}}$, $J_{\Delta a=0}^{\text{Standard}}$ and $J_{\Delta a=0}^{\text{SPT}}$, have been the subject of other studies [15]. A problem which needs to be solved in order to determine the fracture toughness using notched SPT specimens is that of determining the point on the experimental graph where a crack initiates from the notch tip. The initiation point always occurs before attaining the maximum load and can be defined, in a representation of the slope of the load-displacement graph in this region of the curve. Several interrupted laboratory tests were performed at different percentages of the maximum load (95%, 85%, 80% y 75%) in order to verify the initiation of crack growth.

Numerical Simulation of the SPT

Different models have been developed in order to reproduce the SPTs by means of numerical methods. These models were compared with the aim of choosing the optimum model from the point of view of the relation between the precision and the computational cost. The numerical simulations have been carried out with the finite element commercial code ABAQUS [16]. In order to simulate the fracture behaviour of un-notched and notched specimens, two different types of meshes have been used (2D and 3D meshes, respectively). As it was pointed out before, the specimens for laboratory are squared specimens. However, since the hollow between the die and the specimen is a cylinder, the problem can be considered axisymmetric in the un-notched model, and the model can be solved by 2D axisymmetric meshes. In the 2D-Axysim model, the specimens were discretised by means of an axisymmetric mesh of four-node reduced integration hybrid elements. Notwithstanding, since many structural steels are obtained from lamination processes, they exhibit anisotropic

behaviour. In these cases, three-dimensional meshes which reproduced a quarter of the specimen were used (Fig. 6). Although geometries of Fig. 6 appear to be different, the applied boundary conditions allow using both of them for isotropic materials. In this figure, upper die is not represented in order to improve the visualization of the model. In all cases, die and punch were modelled as rigid bodies. Besides, contact between surfaces, quasi-static analysis and large displacements were taken into account.

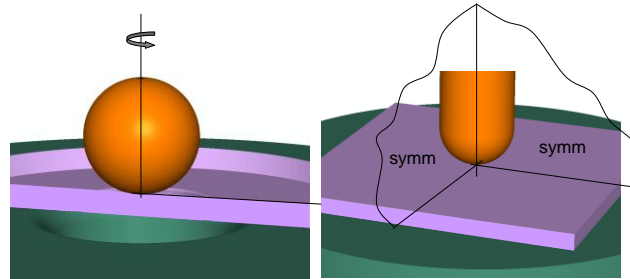


Fig. 6. Axysymmetric and Three-dimensional models used for the simulation of the SPT

From sensitivity analyses, it is observed that the elastic and elastoplastic transition zones are enough to characterize the macromechanical behaviour of steels that exhibit creep behaviour and follow the Hollomon's law ($\sigma=K \cdot \varepsilon_p^n$), whereas the remaining zones allow to characterize the micromechanical behaviour of the material and the coefficient of friction to be used in simulations. A good approximation for the coefficient of friction has been obtained with $\mu = 0.1$, which is also an adequate value for steel–steel contact under partial lubrication. In addition, to describe the evolution of void growth and subsequent macroscopic material softening, the yield function of Gurson–Tvergaard–Needleman [17] was used in this work. The X-70TT material was assumed to be isotropic and its plastic behaviour was adjusted to a power work-hardening law [18] $\sigma=K \cdot \varepsilon_p^n$, where σ is the stress K the strength coefficient of the power hardening law, n the strain hardening exponent ($n \in [0,1]$) and ε_p the plastic strain. The notched specimens were discretised using eight-node reduced integration solid elements. Symmetry was used in these cases in order to reduce the computational cost.

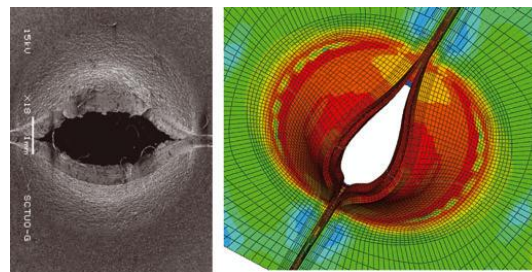


Fig. 7 Comparison of the experimental and numerical deformation shape and fracture zones of a notched SP specimen.

Fig. 7 shows the comparison of deformation and overall appearance of the fracture zone obtained for a notched laboratory specimen and its numerical simulation, for SPT specimen with longitudinal notch. In the case of notched specimens, 3D models has been used. It has been found very good correlation between tests and simulations, not only for the un-notched specimens but also for the notched specimens. The J-integral is widely accepted as a quasi-static fracture mechanics parameter for nonlinear elasto-plastic materials. The J-integral is defined in terms of the energy release rate associated with crack advance. Although the J-integral should be independent of the used integration

path, provided that the faces of the crack are parallel to each other, the J-integral estimates from different contours around the crack may vary because of the approximate nature of the finite element solution. In order to avoid path dependence, in this study the J-integral was obtained in 10 rings and in 18 sections distributed along the notch length. In addition, the integral in each section was determined as the value of the contour integral, which appears approximately constant from one contour to the next.

Results

Given the apparent independence of the geometry of the notch on the fracture behaviour of the notched SP specimen, the numerical and experimental procedure has been repeated again with specimen notched by femtolaser. With this technique, it can be obtained notches tips radius between 1 and 4 μm . The femtolaser is a femtosecond pulsed laser which allows to obtain great accuracy as a result of the minimum volume of material that is affected in each laser pulse Fig. 8 shows a detail of the tip of the notch obtained by this technique. This figure shows also the absence of thermal affection on the lips of the notch after the femtolaser process as well as a good surface finishing on the edges of the notch.

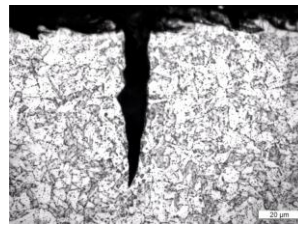


Fig. 8. Detail of the notch tip obtained by femtolaser

Fig. 9 shows the results obtained for micromachining-notched specimens (radius of 100 μm) and for femtolaser-notched specimens (radius of 2 μm) with a notch ratio $a/t = 0.3$ and thickness of 0.5mm. According to the previous results for laser-notched specimens (radius of 10 μm), the results seem to be independent of the technique used for notching the specimen. In addition, the numerical results corroborate this fact.

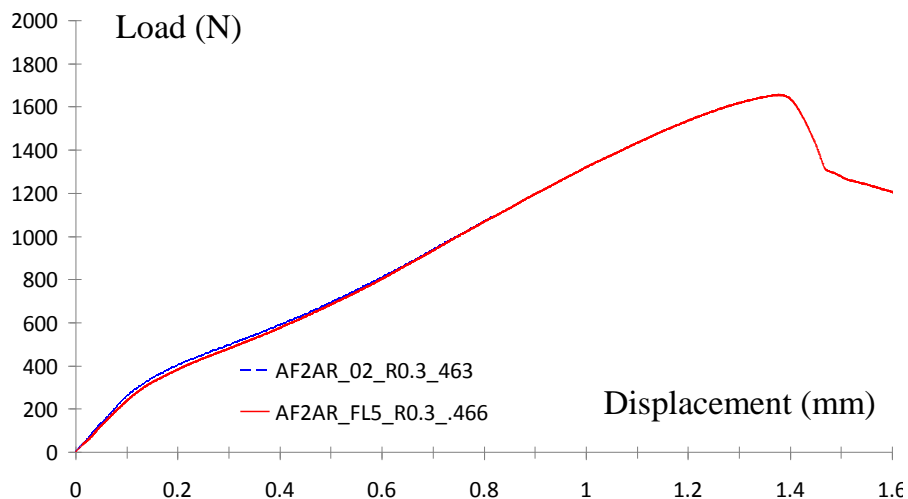


Fig. 9. Load-displacement curve for the micromachined and femtolaser notched specimens

Conclusions

In previous works, the authors of the paper have shown that the SPT can be used to characterized not only the conventional mechanical properties, but also the fracture toughness. In order to calculate this latest property directly, it has been necessary to use notched small punch test specimens.

In the present paper, has shown that the despite the great influence of the relative depth of the notch (a/t) in the fracture behaviour of the specimen, the geometry of the tip of the notch has no influence on the fracture of the specimen, as a consequence of the characteristic stress state at the notch tip. This fact has been observed for different materials which exhibit different behaviour (ductile, transition or brittle), not only at room temperature, bur also for low temperatures. Therefore, in the sake of simplicity, and taken into account: 1) the better control of the notching process in the case of micromachining, in which the notch obtained along the specimen is totally uniform in comparison with other laser techniques (either laser or femtolaser) where the initial and final zones of the notch exhibit differences compared to the central zones of the specimen, as well as less uniformity in the surface finish , 2) the higher difficulty of controlling the relative depth of the notch in the case of laser notched specimens and finally 3) the economical aspect – the cost of micromachine-notched specimens is much smaller than that of the laser-notched or femtolaser-notched ones-, it is recommended using the micromachining technique versus laser techniques for determining the fracture behaviour of notched SPT specimens.

References

- [1] Lucas G.E. et al., J. Nucl. Mater., Vol. 307-311 (2002) p. 1600-1608,.
- [2] Lucon E., Mater. Scie. Tech., Vol. 17 (2001), p. 777-785.
- [3] Peñuelas I. et al., Actas del IX congreso iberoamericano de Ingeniería Mecánica, (2009).
- [4] Li, J. et al., Funtai Oyobi Fummatsu Yakin/Journal of the Japan Society of Powder and Powder Metallurgy, Vol. 45 (1998), p. 237–241.
- [5] Rodríguez, C. et al., Welding Journal Vol. 88 (2009), p.188s–192s.
- [6] Suzuki, M. et al., J. Nucl. Mater., Vol. 179–181, Part 1 (1991) p. 441–444.
- [7] Contreras MA., PHD. Tesis, University of Oviedo, (2007).
- [8] Autillo J. et al., Anales de Mecánica de la Fractura, Vol. 23 (2006), p. 77-83.
- [9] Contreras M.A. et al., Fatigue Fract Engng Mater Struct, Vol. 31 (2008), p. 727-737.
- [10] Mao X., H. Takahashi and T., Materials Science and Engineering, AI50 (1992), p. 231-236.
- [11] Shekhter A. et al., International Journal of Pressure Vessels and Piping Vol. 79 (2002.), p. 611–615.
- [12] Peñuelas I. et al., Anales de Mecánica de la Fractura, 27, 503-507, 2010.
- [13] Cárdenas E. et al., Fatigue and Fracture of Engineering Materials and Structures, doi: 10.1111/j.1460-2695.2011.01635.x, 2012.
- [14] Peñuelas I. et al., Fatigue and Fracture of Engineering Materials & Structures, Vol. 32 (2009), p. 872-885.
- [15] ASTM E1820 (1999) Standard test method for measurement of fracture toughness ASTM International, West Conshohocken, Pensilvania, USA.
- [16] ABAQUS 6.10., Hibbit, Karlsson and Sorensen, Inc., Pawtucket, 2010.
- [17] Tvergaard V, Needleman A. Acta Metall. Vol. 32 (1984), p. 57-169.
- [18] Dowling, N. E. In: *Mechanical Behaviour of Materials*. Edited by Prentice Hall, Upper Saddle River, New Jersey, USA (1999).